Multipactor Phenomenon in Dielectric-Loaded Accelerating Structures: Review of Theory and Code Development

O. V. Sinitsyn, G. S. Nusinovich and T. M. Antonsen, Jr.

IREAP, University of Maryland, College Park, MD 20742

3rd International Workshop on Mechanisms of Vacuum Arcs
1-4 Oct. 2012, Albuquerque, NM, USA

University of Maryland 1856
Institute for Research in Electronics & Applied Physics

Outline

- What is multipactor?
- Experimental observation of MP in DLA structures
- Theoretical models
- Code development
- Summary

What is multipactor?

- Avalanche growth of the number of free electrons emitted from a solid surface in the presence of RF field under vacuum conditions.
- It occurs in various RF and microwave systems: microwave tubes, rf windows and launchers, accelerating structures, satellite RF systems.
- MP generates RF noise, reduces RF power flow, changes device impedance, stimulates RF breakdown etc.
- MP may occur in different situations: single- and two-surface, on the surface of metals and dielectrics, where RF electric field is normal, tangential or combination of both.

Different types of MP

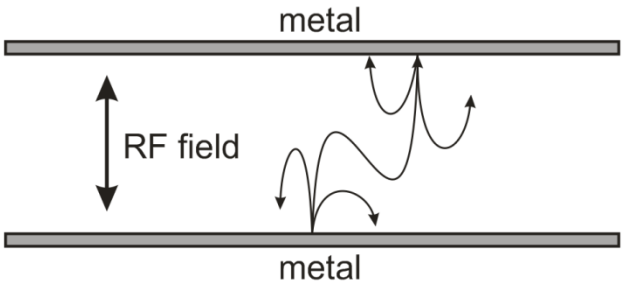

Two-surface MP between two parallel metal plates (waveguides, transmission lines)

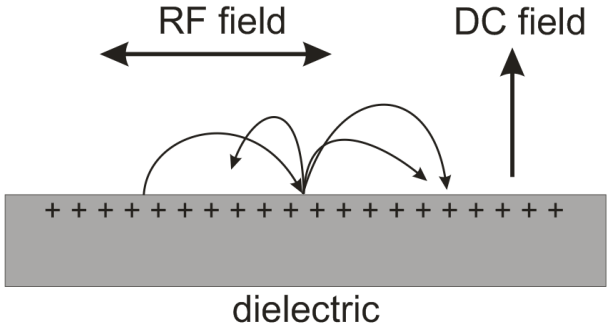

Single surface MP on a dielectric (RF windows)

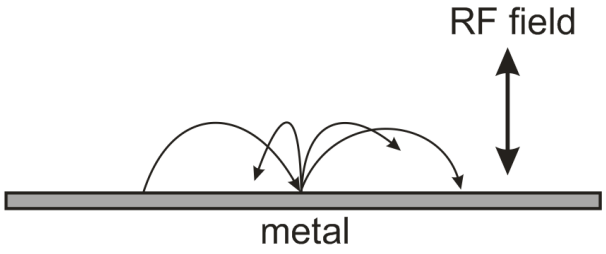

Single-surface MP on a metal surface (various RF components)

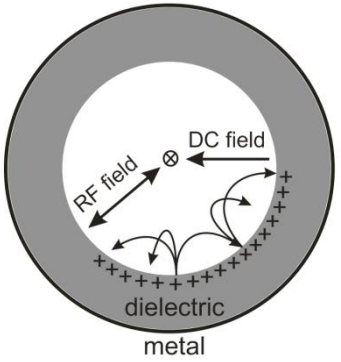

MP in dielectric-loaded accelerating structures

DLA structures

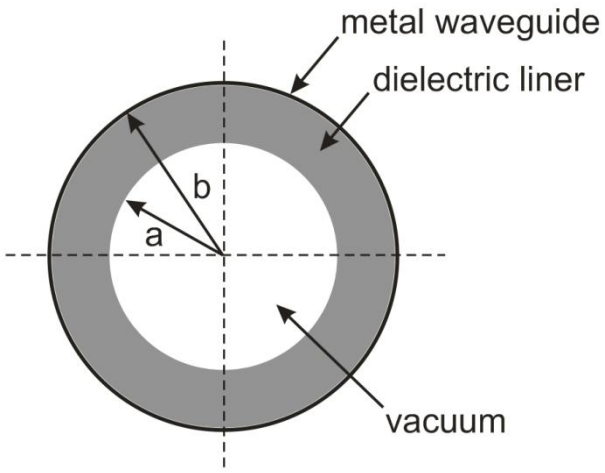

Cross-section of a cylindrical DLA structure

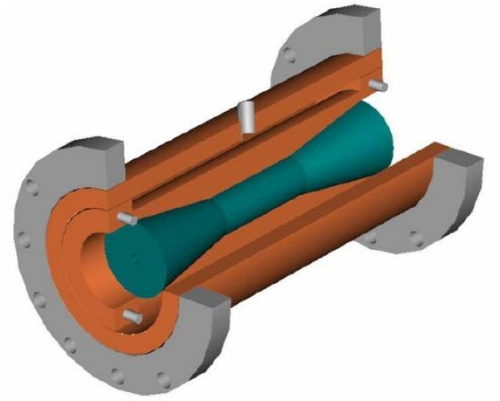

3D view of the DLA structure

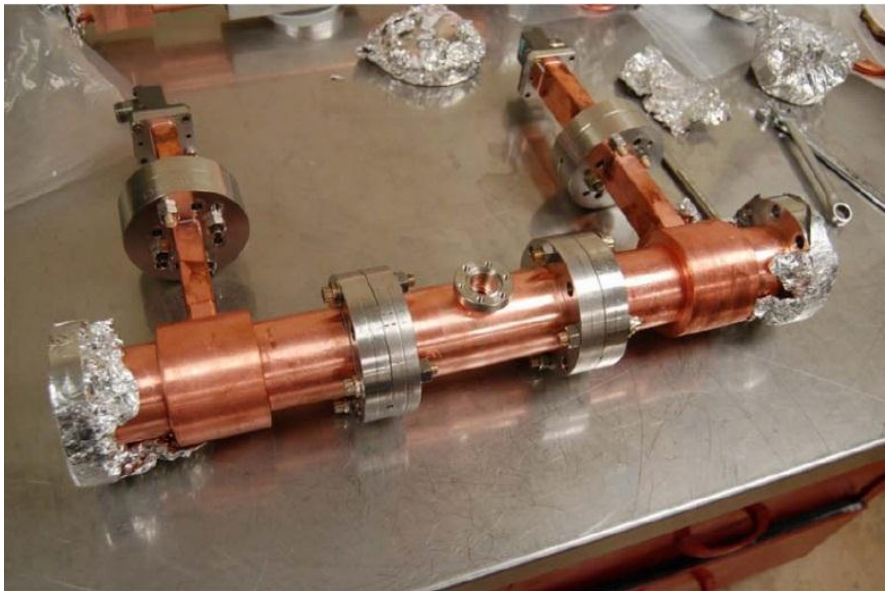

Assembled clamped DLA structure using TE_{10} - TM_{01} high-power RF couplers (C. Jing et al., IEEE Trans. Plasma Sci., 38, No. 6, 2010)

Experimental studies of MP at ANL and NRL

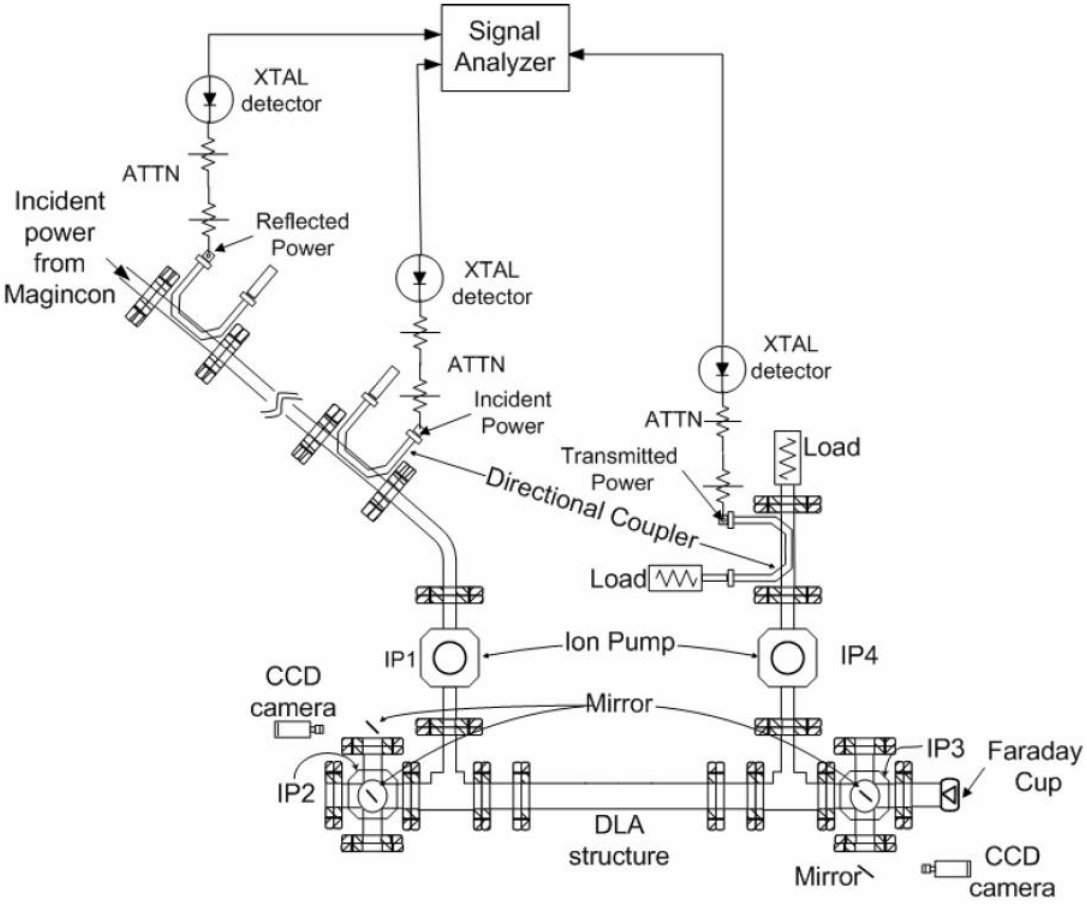

Experimental setup used to test DLA structures with high-power RF. X-band Magnicon at NRL powered the traveling-wave DLA structure. Three bidirectional couplers used to detect incident, reflected and transmitted power, ion pumps controlled vacuum and the CCD cameras were used to observe arcing inside the tube (C. Jing et al., AIP Conf. Proc., 737, 258 (2004)).

Experimental observation of MP in DLA structures

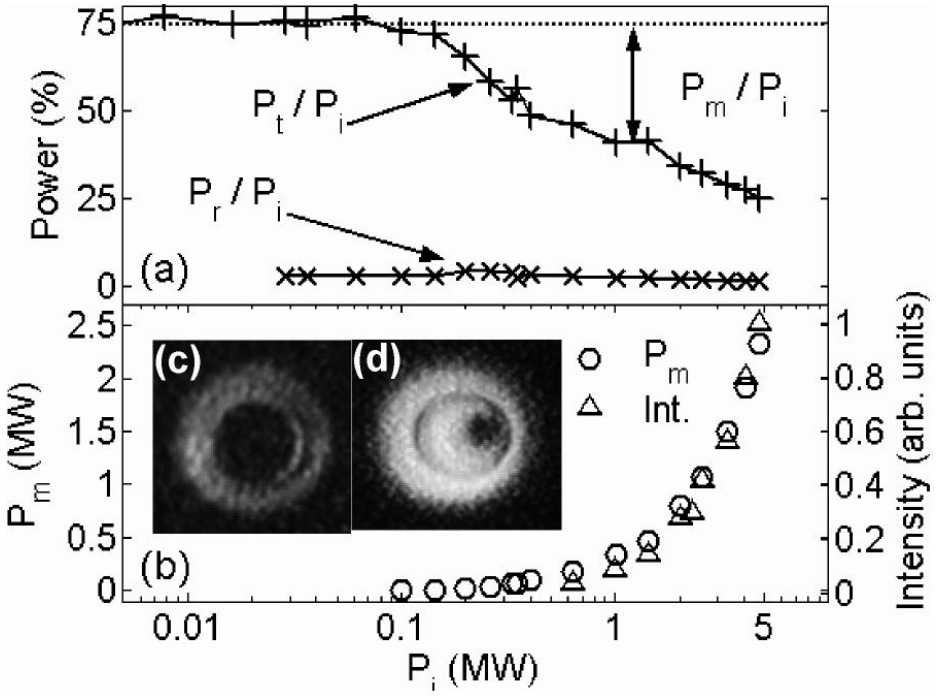

TABLE I
GEOMETRIC AND PHYSICAL PROPERTIES OF THE 11.424-GHZ ALUMINA BASED DLA STRUCTURE

PARAMETERS	VALUE
Material	Alumina
Dielectric constant	9.4
Inner radius	5mm
Outer radius	7.185mm
R/Q	6.9kΩ/m
Group velocity	0.134c
RF power needed to support 1MV/m gradient	80kW

Measured values of (a) the transmission and reflection coefficients and (b) the missing power and the time-integrated light intensity as a function of incident power. (c),(d) Images of light observed during the high-power test of the alumina DLA structure. (J. G. Power et al., PRL, 92, 164801 (2004)).

Experimental observation of MP in DLA structures

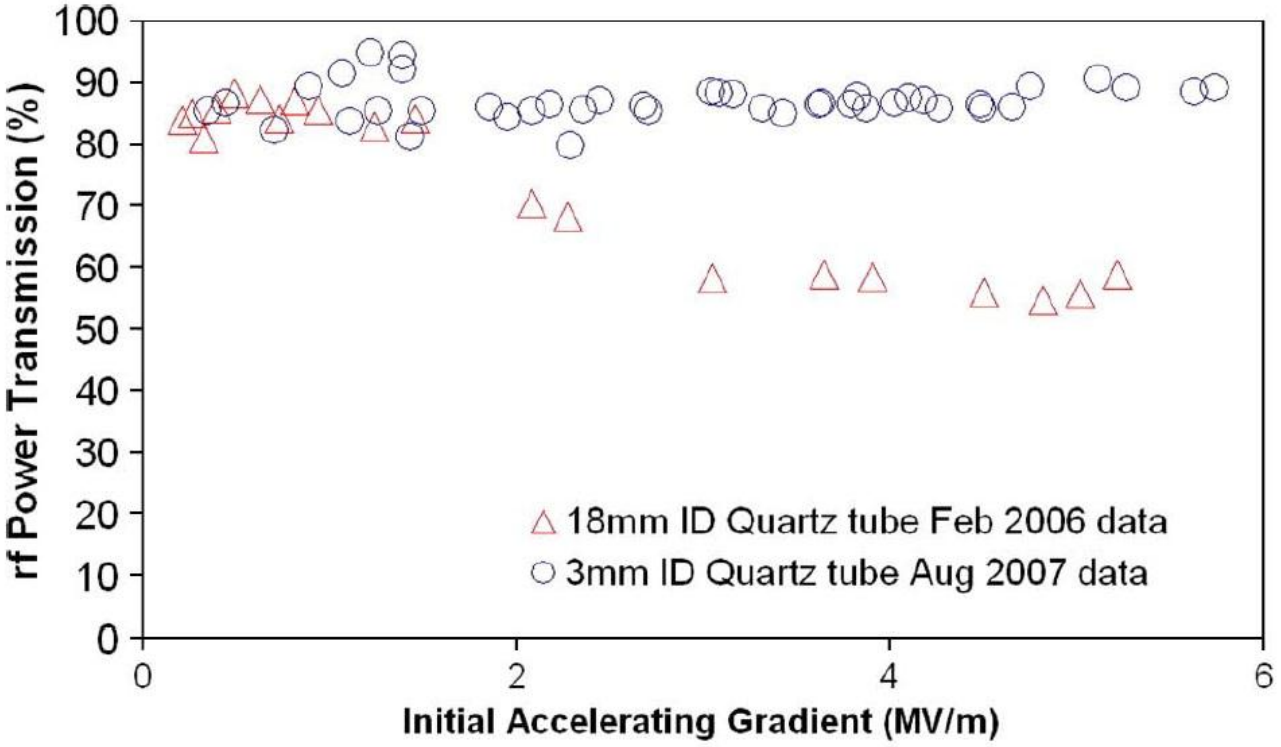

RF power transmission vs accelerating gradient for two quartz-based DLA structures with different inner diameters (C. Jing et al., IEEE Trans. Plasma Sci., 38, No. 6, 2010)

MP suppression by TiN coating

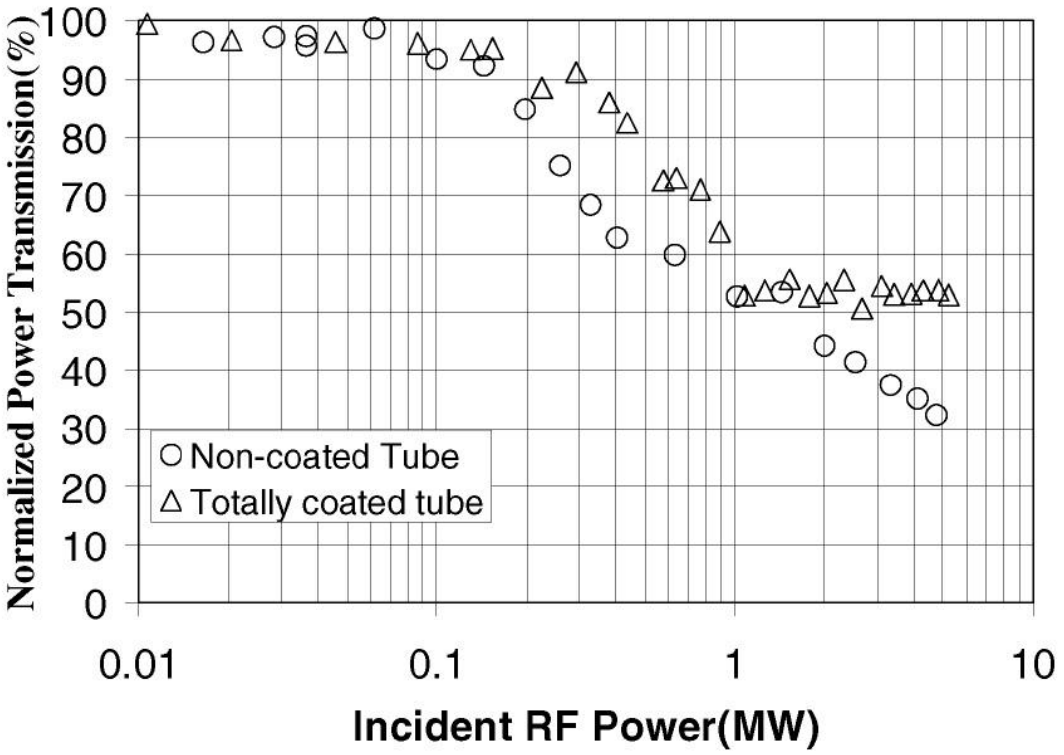

In order to suppress MP in the alumina-based DLA structure, the inner surface of the tube was coated with 20 nm-thick TiN film. TiN is commonly used for lowering the secondary emission yield in high-power RF window applications (C. Jing et al, IEEE Trans. Plasma Sci., 33, p. 1155 (2005)).

Theoretical studies of MP

Theoretical single surface model of MP with both normal and tangential RF fields and normal SC field used by J. Power et al. (AIP Conf. Proc., 877, 362 (2006)).

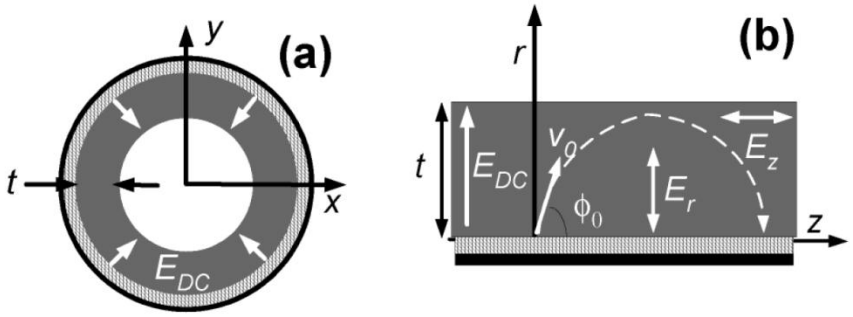

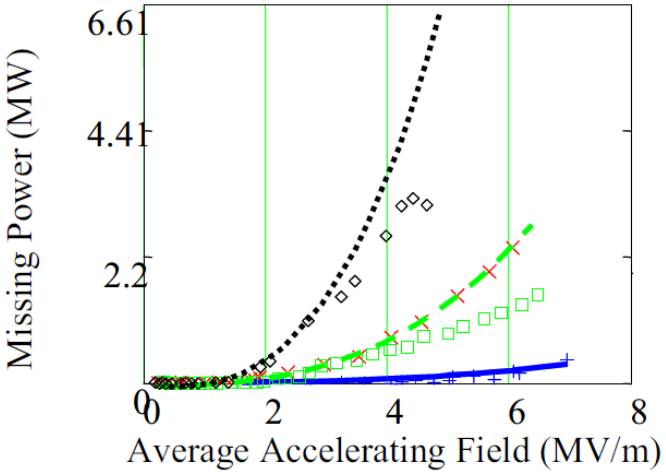

Fused silica – diamonds, alumina – X, coated alumina – squares, MCT-20 - +

Model assumptions:

- Particles are emitted normal to the surface and are monoenergetic
- MP is driven mainly by the radial component of the RF field, z motion is ignored
- Particles experience space charge field E_{SC} normal to the surface (used as a parameter)
- MP is resonant, it takes one RF period for the particle to return to the surface

Motivation for our work

- In order to correctly model MP at saturation, E_{SC} should be calculated self-consistently
- Real particles are emitted with random initial energies and emission phases
- It is not clear whether MP in DLA structures is resonant or it can have some different features.
- A more sophisticated Monte-Carlo model was needed.

1-D model of MP

- Flat model, no effects of cylindricity
- Effects of E_z are neglected, no axial motion of particles
- No RF magnetic field

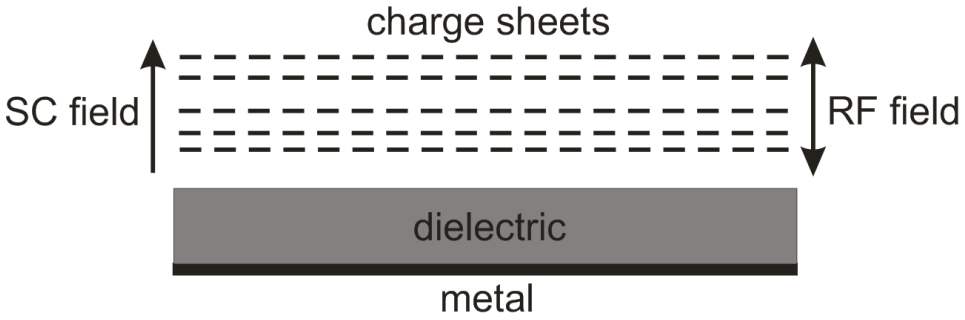

Equation of electron motion:

$$m\ddot{r} = -e(E_{RF} + E_{SC})$$

Radial component of the RF field (TM_{01} mode) near the dielectric surface

$$E_{RF} = -A\frac{k_z a}{2}\sin(\omega t + \psi)$$

Space charge field calculation

$$E_{SC} = \frac{\sigma_0}{\varepsilon_0}\sum_n w_n$$

1-D model of MP

- Particles are emitted with random initial energies and phases
- Secondary emission yield (SEY) is calculated by using Vaughan's model

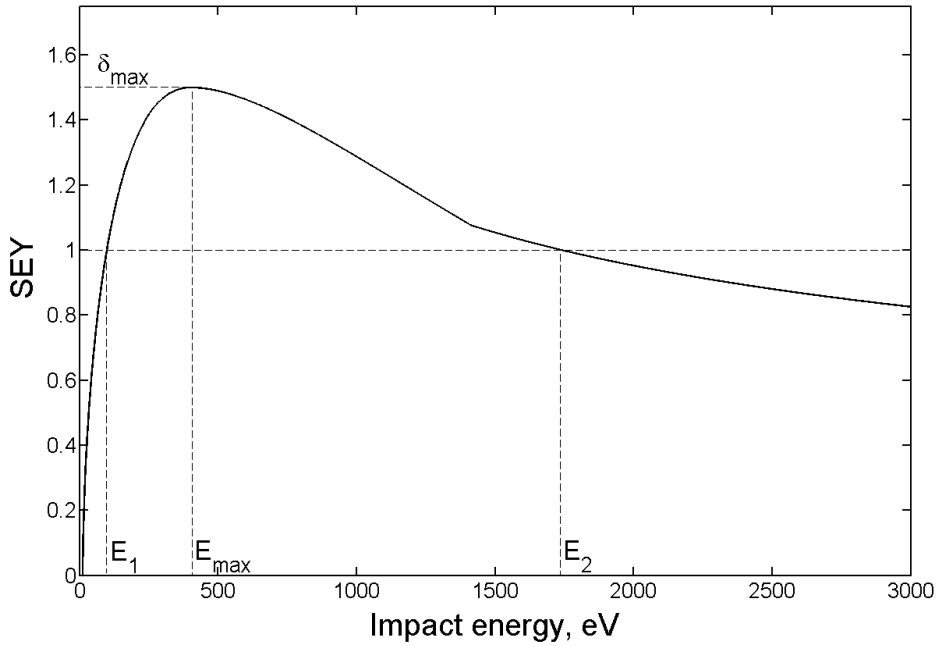

- In the 1-D case SEY model is characterized by 3 parameters: E_i – impact energy, δ_{max} – max secondary yield and E_{max} – energy corresponding to δ_{max}.

Simulation results

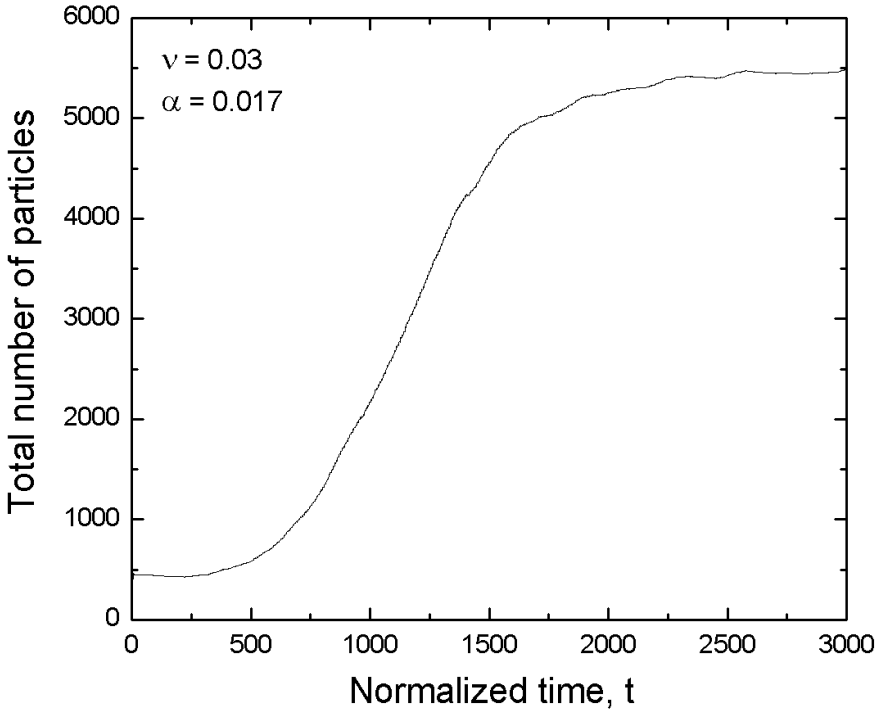

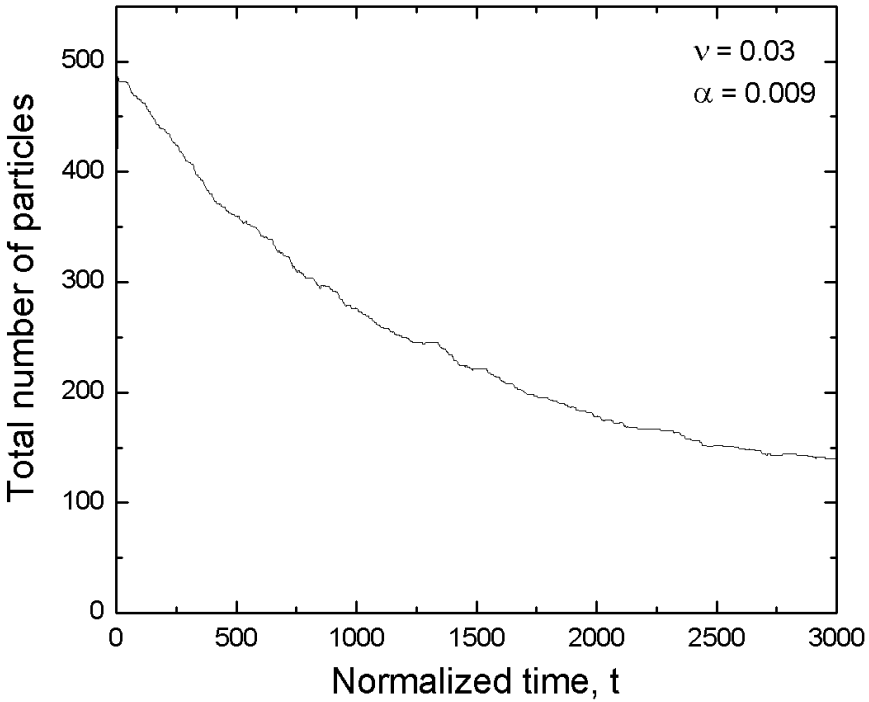

Total number of macroparticles vs normalized time for two values of the normalized RF amplitude α. MP occurs on the first plot, no MP on the second plot.

Shortcomings of 1-D model

- Given sufficient initial energies, the electrons may travel far away from the dielectric surface and never return. This is impossible in real life since their radial position can only change between 0 and dielectric surface.
- The returning force due to SC field acts on the particles that are closer to the dielectric surface, however the particles that are further away experience weak or no SC effect.
- We tried to limit the particle motion by imposing conditions for particle reflection at r = 0, however this resulted in incorrect calculations of saturation levels.
- The particles could leave and arrive to the dielectric surface only at normal which resulted in diminished values of SEY.
- More sophisticated model was needed.

2-D model of MP

- Effects of cylindricity included
- Particles have random emission angles in $r-\varphi$ plane
- Effects of E_z are neglected, no axial motion of particles

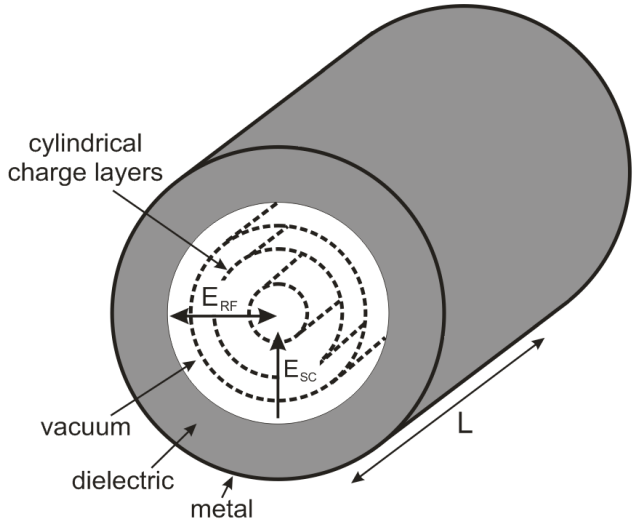

Equations of electron motion:

$$\frac{dv_r}{dt} = \frac{v_\varphi^2}{r} - \frac{e}{m}(E_{SC,r} + E_{RF,r})$$

$$\frac{dv_\varphi}{dt} = -\frac{v_r v_\varphi}{r}$$

$$\frac{dr}{dt} = v_r, \quad \frac{d\varphi}{dt} = \frac{v_\varphi}{r}$$

RF electric field radial component:

$$E_{RF,r} = -A\frac{k_z}{k_{\perp 1}} I_1(k_{\perp 1} r)\sin(\omega t + \psi)$$

2-D model of MP

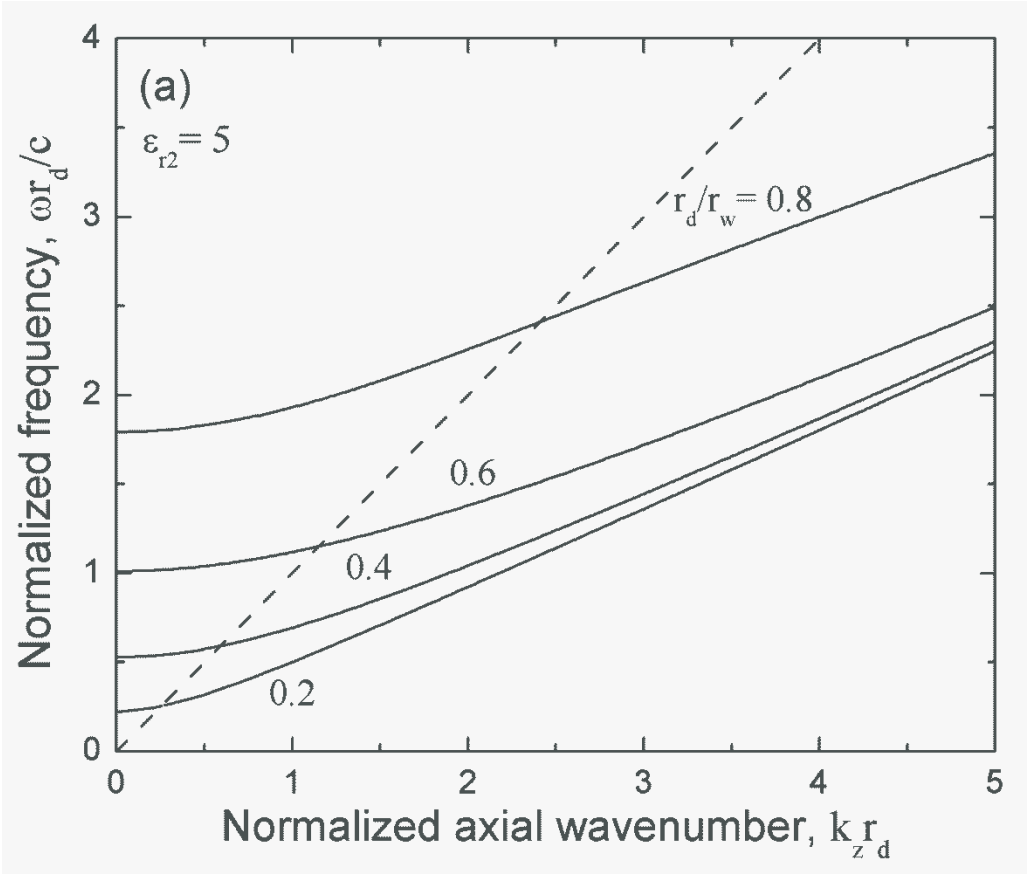

Axial and transverse wavenumbers can be obtained from the dispersion equation for the dielectric-loaded waveguide.

2-D model of MP

- SC field calculation with Gauss law:

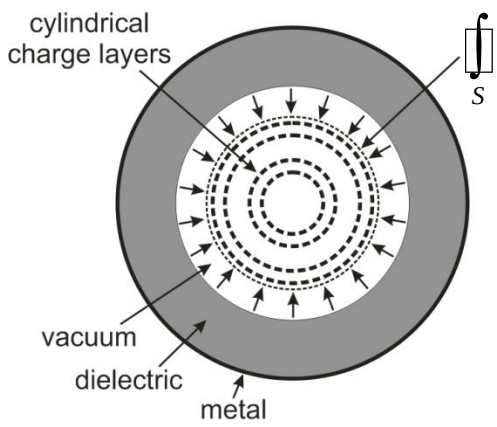

$$\oint_S \vec{E} d\vec{S} = \frac{Q}{\varepsilon_0}$$

E_{SC} outside n-th layer:

$$E^n_{SC,r}(r) = \frac{a\sigma_0}{r\varepsilon_0}\sum_{m=1}^{n} w_m$$

$$\sigma_0 = -\frac{eN_0}{2\pi aL}$$

w_m - relative weight of m-th layer,
σ_0- initial particle surface density

- SEY calculation:

Dependence of SEY on impact angle included in 2-D

$$E_{\max}(\theta_i) = E_{\max 0}(1 + k_{sV}\theta_i^2 / 2\pi)$$

$$\delta_{\max}(\theta_i) = \delta_{\max 0}(1 + k_{s\delta}\theta_i^2 / 2\pi)$$

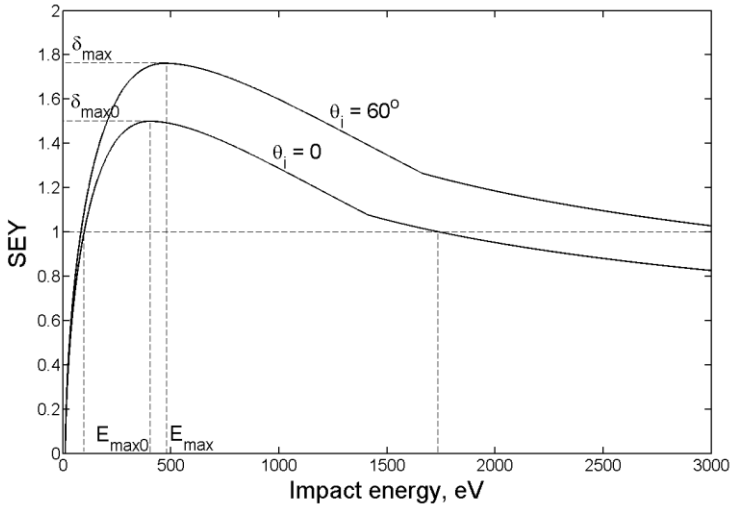

Simulation results

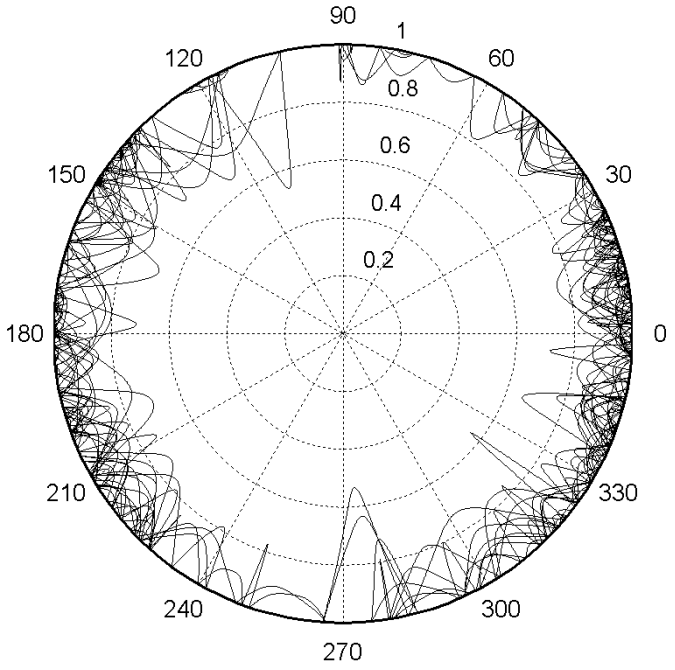

Sample particle trajectories for 3 MV/m accelerating gradient

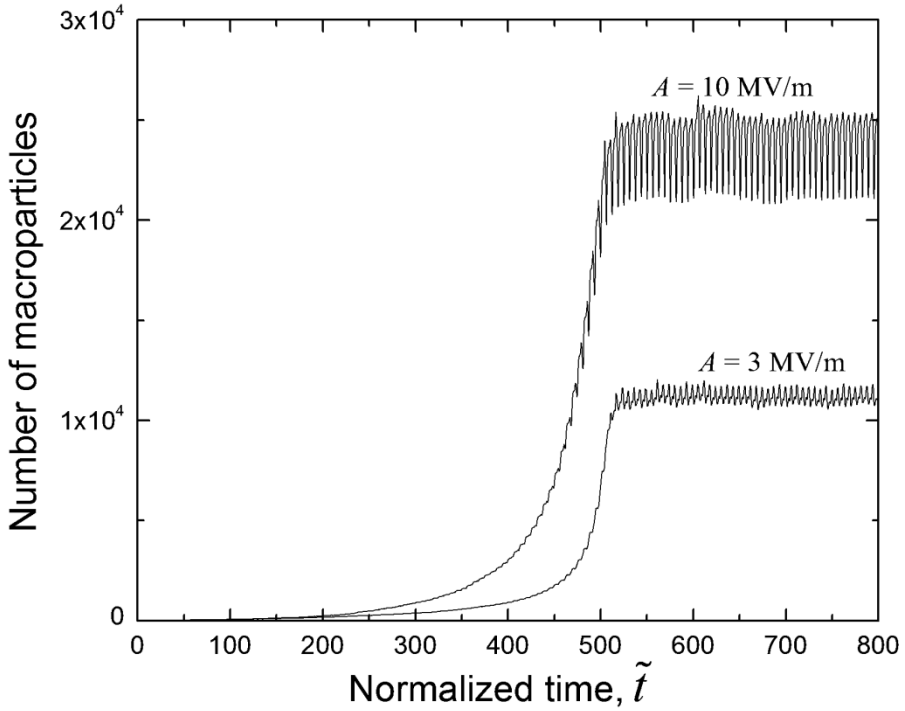

Number of macroparticles vs time for two values of the accelerating gradient

(O. V. Sinitsyn et al., Phys. Plasmas, 16, 073102 (2009))

Comparison with experiment

We were modeling 4 structures that had been tested experimentally

DLA structure	a, mm	b, mm	ε_r	δ_{max0}	E_{max0}, eV
Alumina-based	5.0	7.185	9.4	1.5 – 9.0	350-1,300
Quartz-based	8.97	12.08	3.75	2.4 – 3.0	400
Quartz-based	3.0	7.372	3.75	2.4 – 3.0	400
Quartz-based	1.5	6.47	3.75	2.4 – 3.0	400

2-D model vs experiment

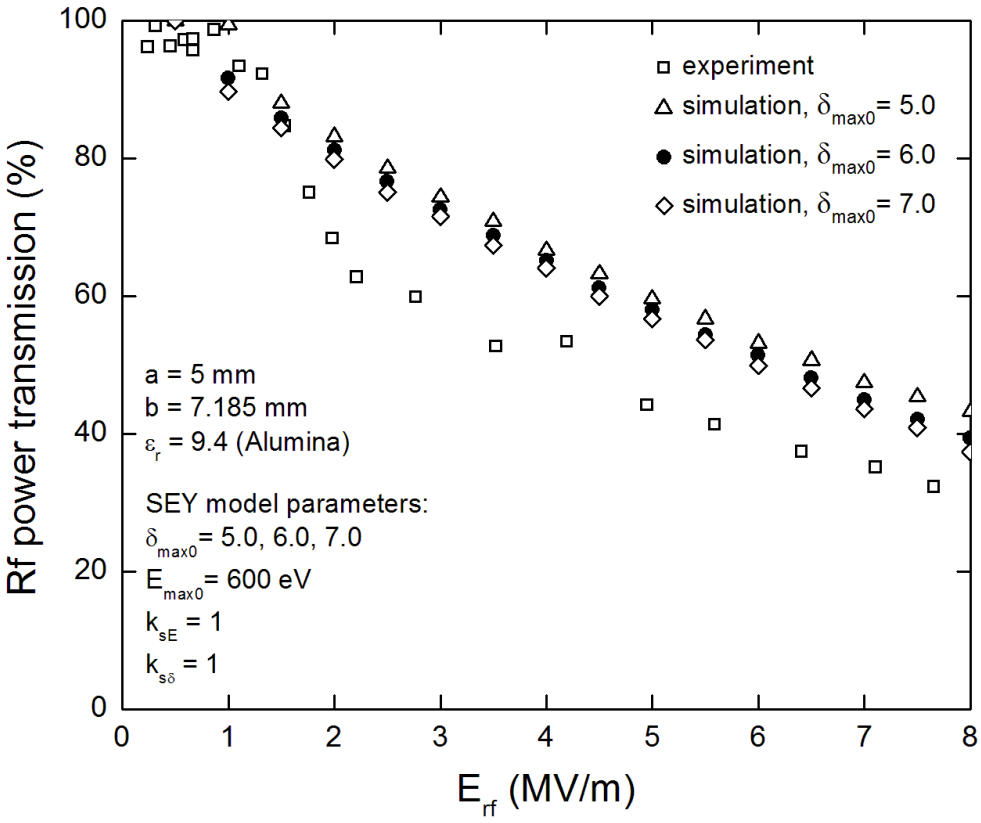

RF power transmission vs acceleration gradient for alumina-based DLA structure with inner diameter = 10 mm
(O. V. Sinitsyn et al., AAC 2010 Workshop,
AIP Conf. Proc., 1299, pp. 302-306, 2010)

2-D model vs experiment

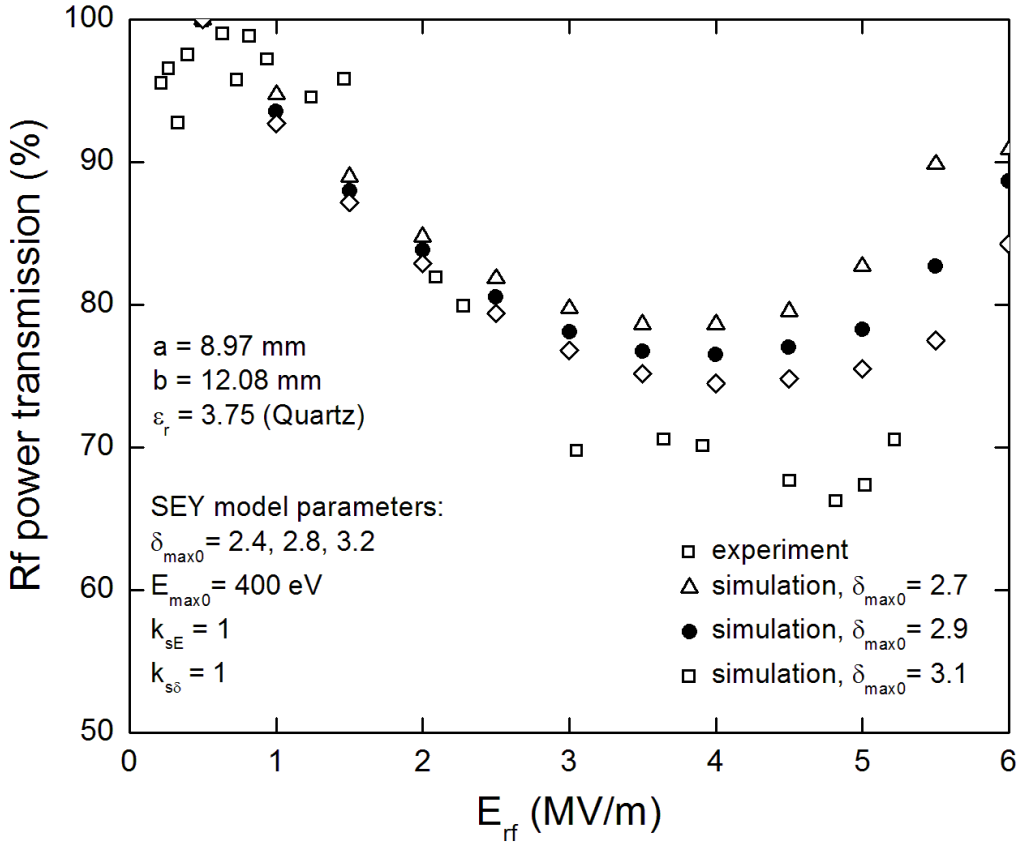

RF power transmission vs acceleration gradient for quartz-based DLA structure with inner diameter = 18 mm

2-D model vs experiment

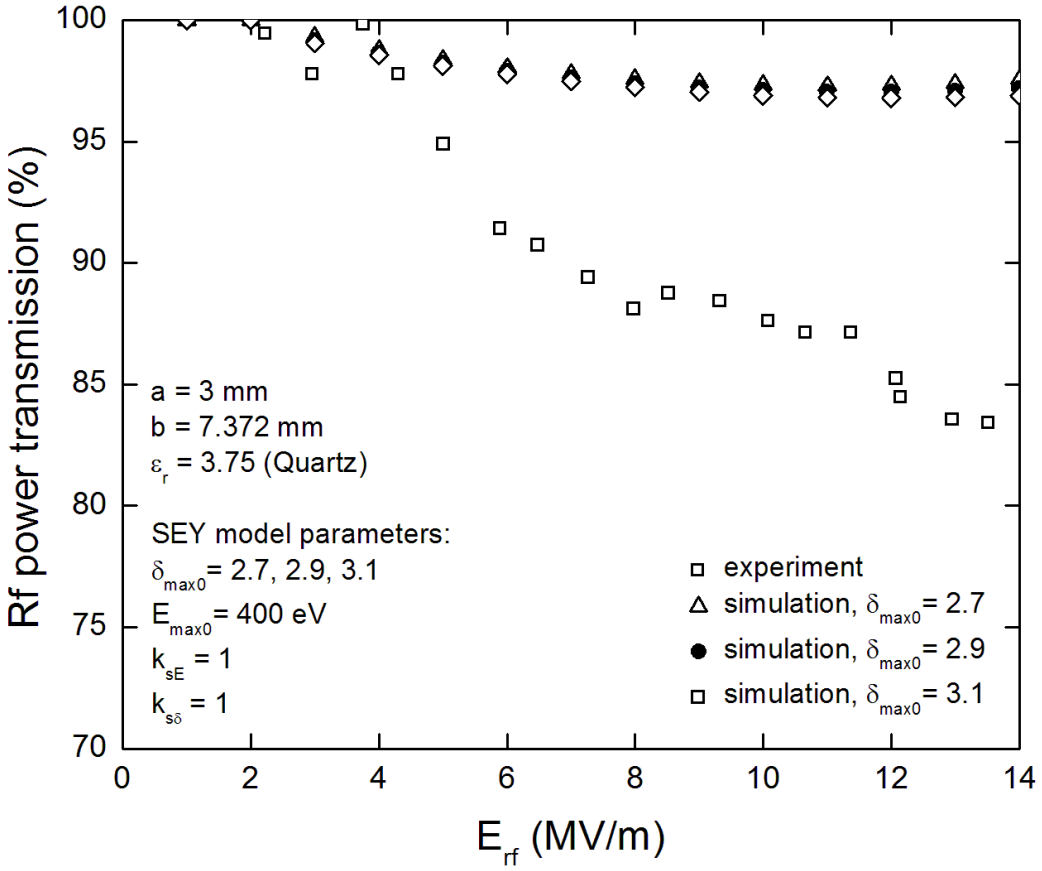

RF power transmission vs acceleration gradient for quartz-based DLA structure with inner diameter = 6 mm

Shortcomings of the 2-D model

- Bad agreement between simulation and experimental data for structures with small inner diameter
- Axial motion of particles was not taken into account, which could be the reason for the discrepancy.
- MP-induced loss was not calculated self-consistently
- 3-D model of MP was needed.

3-D model of MP

- Axial motion of particles included
- Improved calculation scheme for E_{SC}
- Self-consistent calculation of MP-induced power loss

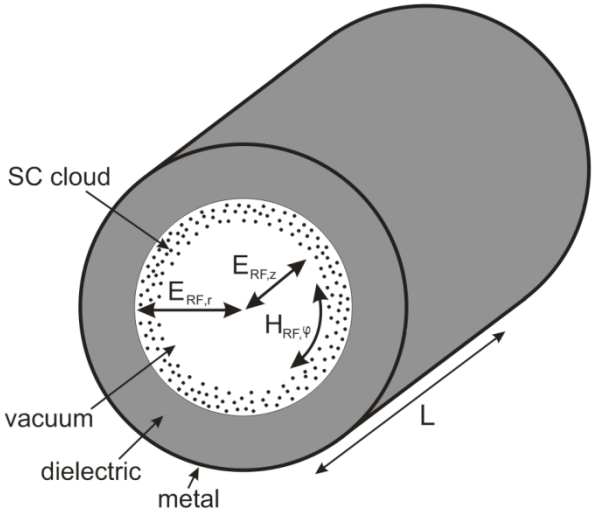

$$\frac{dv_r}{dt} = \frac{v_\varphi^2}{r} - \frac{e}{m}\left(E_{RF,r} + E_{SC,r} - v_z B_{RF,\varphi}\right)$$

$$\frac{dv_\varphi}{dt} = -\frac{v_r v_\varphi}{r} - \frac{e}{m}\left(E_{SC,\varphi} - v_r B_z\right)$$

$$\frac{dv_z}{dt} = -\frac{e}{m}\left(E_{RF,z} + E_{SC,z} + v_r B_{RF,\varphi}\right)$$

RF field components (TM_{01} mode)

$$E_{RF,z} = AI_0(k_{\perp 1} r)\cos(\omega t - k_z z)$$

$$E_{RF,r} = -A(k_z / k_{\perp 1}) I_1(k_{\perp 1} r)\sin(\omega t - k_z z)$$

$$H_{RF,\varphi} = -A\left(\omega\varepsilon_0 / k_{\perp 1}\right) I_1(k_{\perp 1} r)\sin(\omega t - k_z z)$$

3-D model of MP

- SC field calculation:

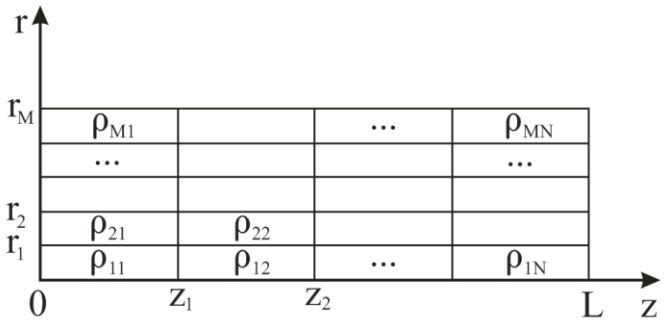

$$E_{SC,r}^{m,n}(r)=\frac{1}{2\varepsilon_0}\left(\frac{1}{r}\sum_{l=2}^{m}r_{l-1}^2(\rho_{l-1,n}-\rho_{l,n})+r\rho_{m,n}\right),\quad m\geq 2$$

$$E_{SC,r}^{1,n}(r)=\frac{\rho_{1,n}r}{2\varepsilon_0},\qquad m=1$$

$$\rho_{m,n}=Q_{m,n}/V_m,\quad Q_{m,n}=-q_0\sum_k w_k$$

- MP-induced wave attenuation:

$$p_k=-e\sum_i v_{k,i}(E_{RF,i}+E_{SC,i})$$

$$P_{MP,n}=n_0\sum_k w_{n,k}p_{n,k}$$

$$P_{RF,n+1}=P_{RF,n}-P_{MP,n}$$

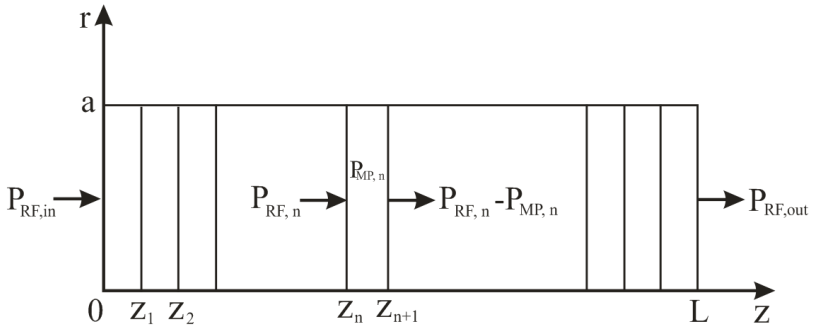

3-D model of MP

- Secondary electrons energy distribution

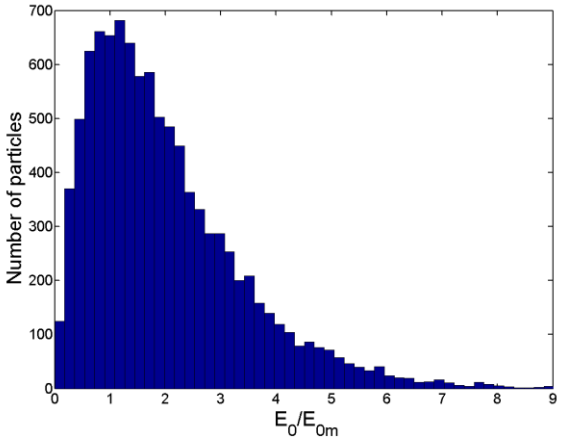

$$f(E_0) = \frac{E_0}{E_{0m}^2} \exp\left(-\frac{E_0}{E_{0m}}\right)$$

$$E_{0m} = 3 - 5\, eV$$

- Distribution of emission angles:

$$f(\theta_e) = \frac{1}{2}\cos(\theta_e)$$

Particles have the same distribution function for emission angles in both $\varphi - r$ and $z - r$ planes.

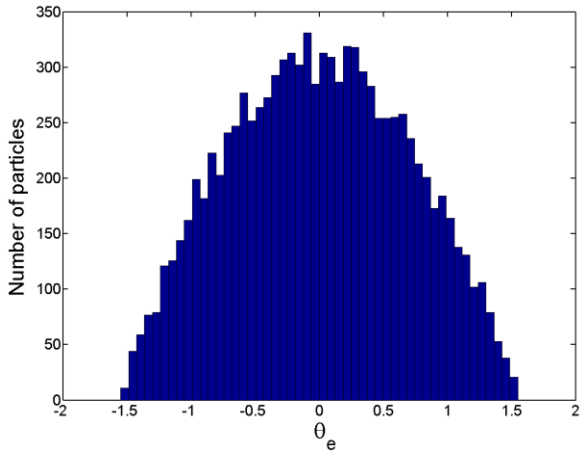

Simulation results

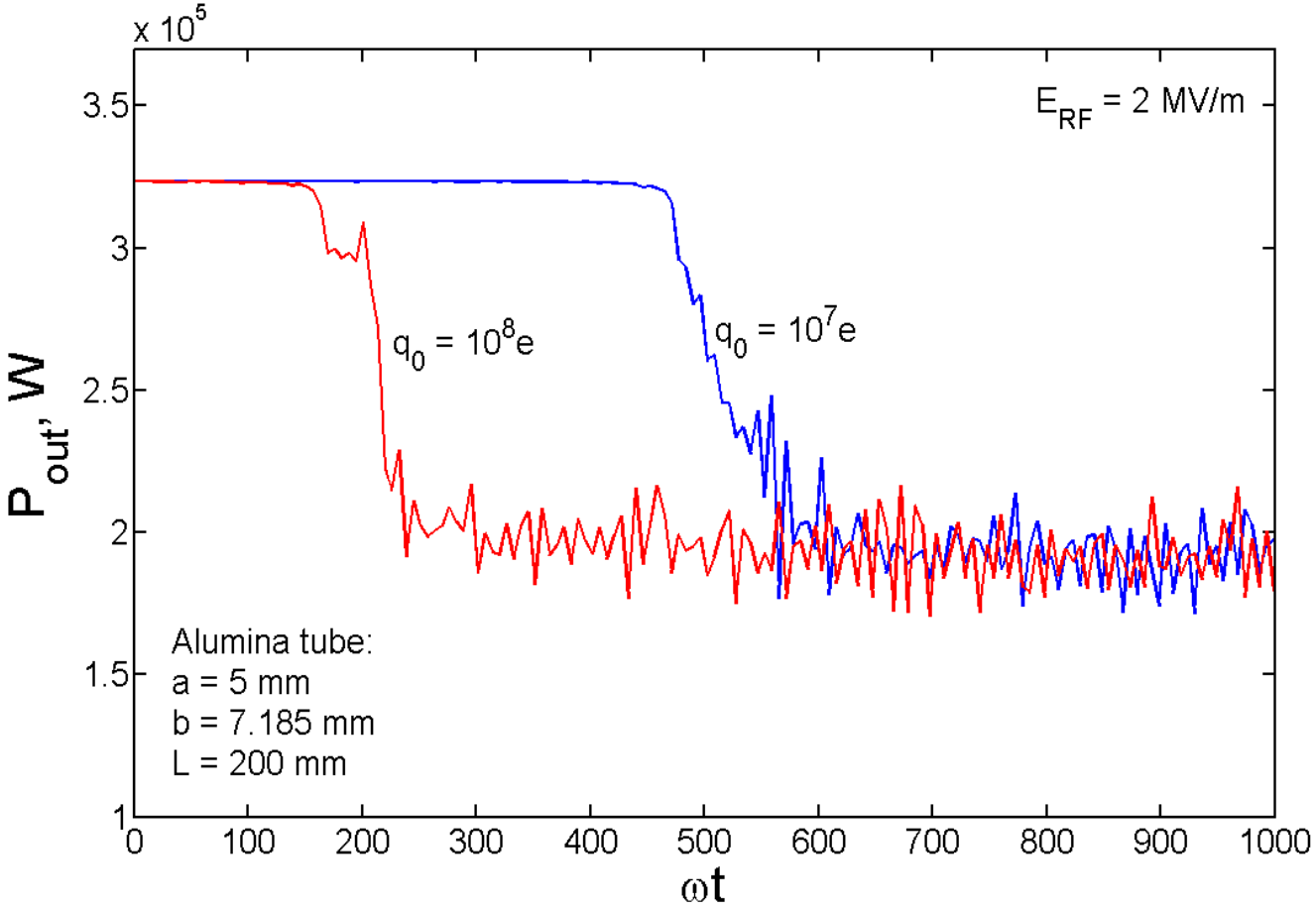

Output power vs normalized time for the alumina-based DLA structure computed for two values of the initial charge carried by each macroparticle.

3-D model vs experiment

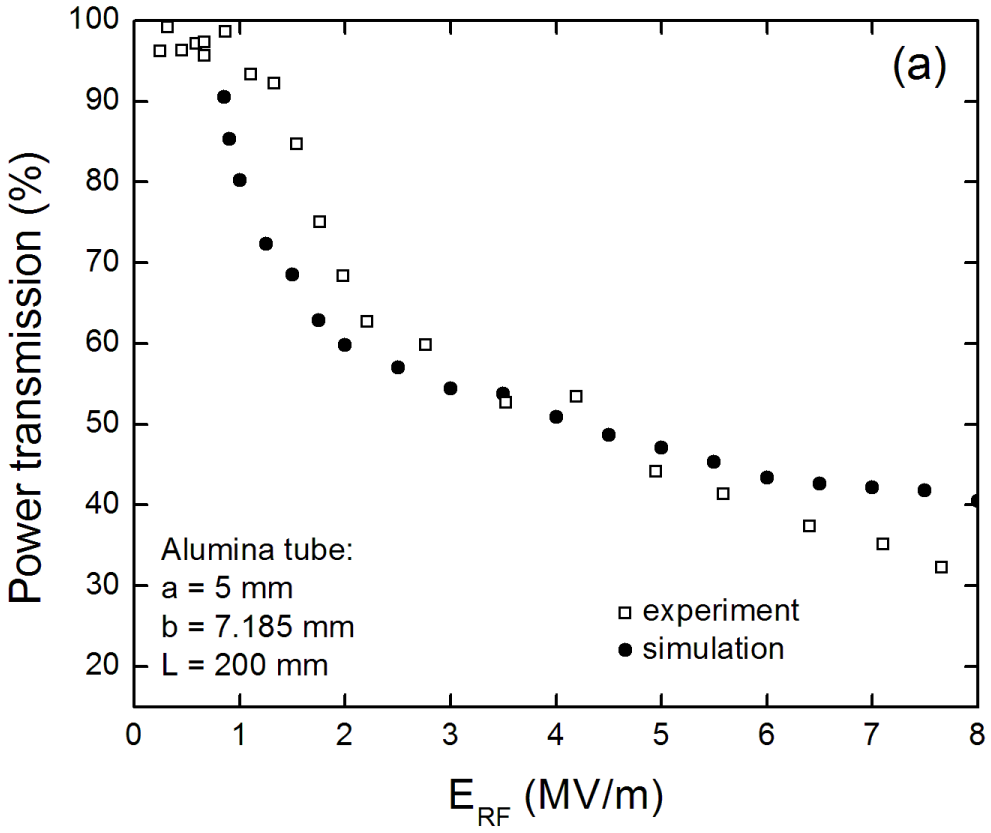

RF power transmission vs acceleration gradient for alumina-based DLA structure with inner diameter = 10 mm, SEY model: δ_{max0}= 6, E_{max0}=600 eV. (O. V. Sinitsyn et al., AAC 2012 Workshop, Austin, TX, USA)

3-D model vs experiment

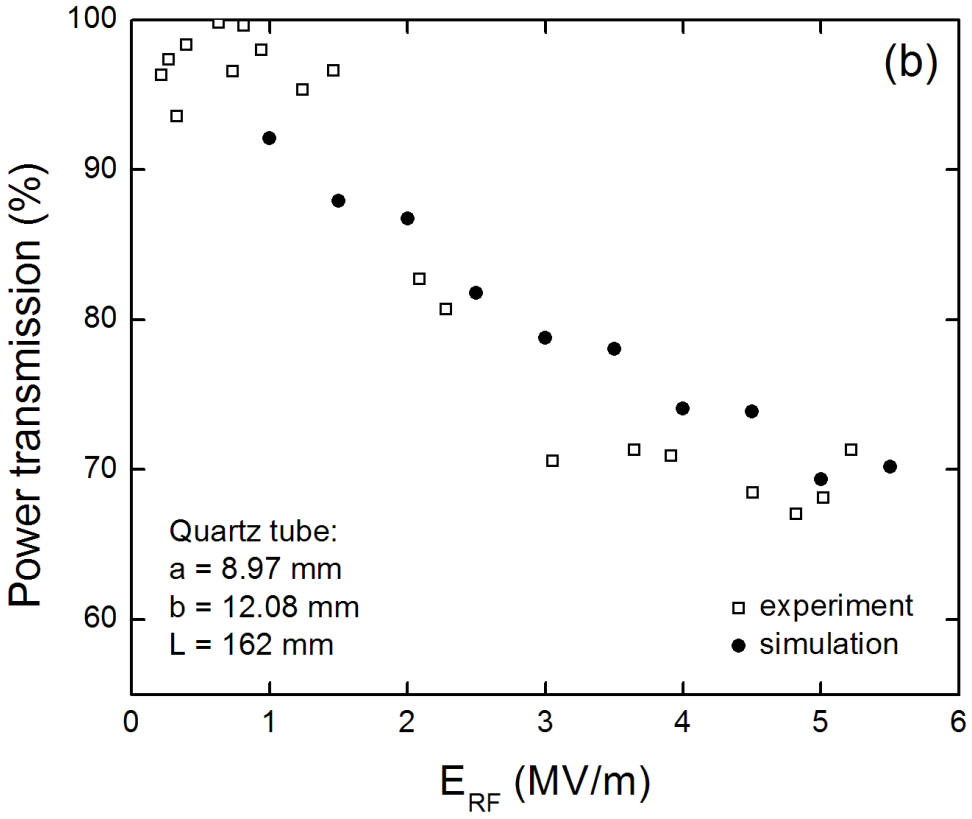

RF power transmission vs acceleration gradient for quartz-based DLA structure with inner diameter = 18 mm, SEY model: δ_{max0}= 2.4, E_{max0}=400 eV.

3-D model vs experiment

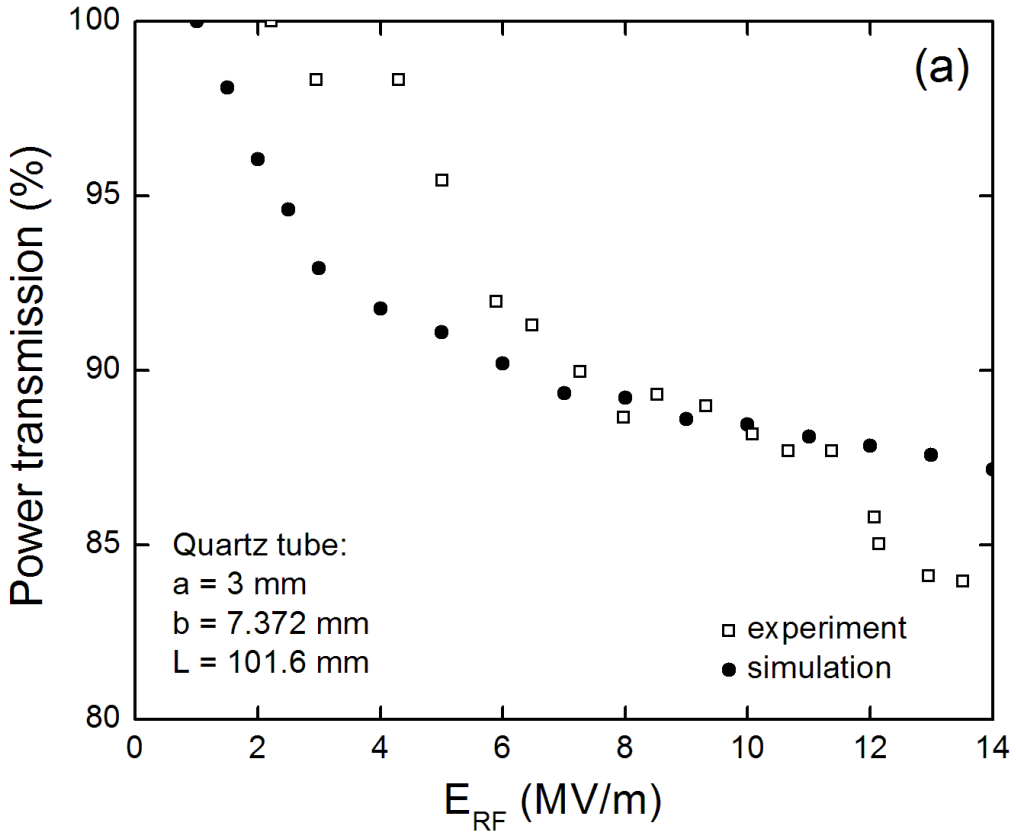

RF power transmission vs acceleration gradient for quartz-based DLA structure with inner diameter = 6 mm, SEY model: δ_{max0}= 2.4, E_{max0}=400 eV.

3-D model vs experiment

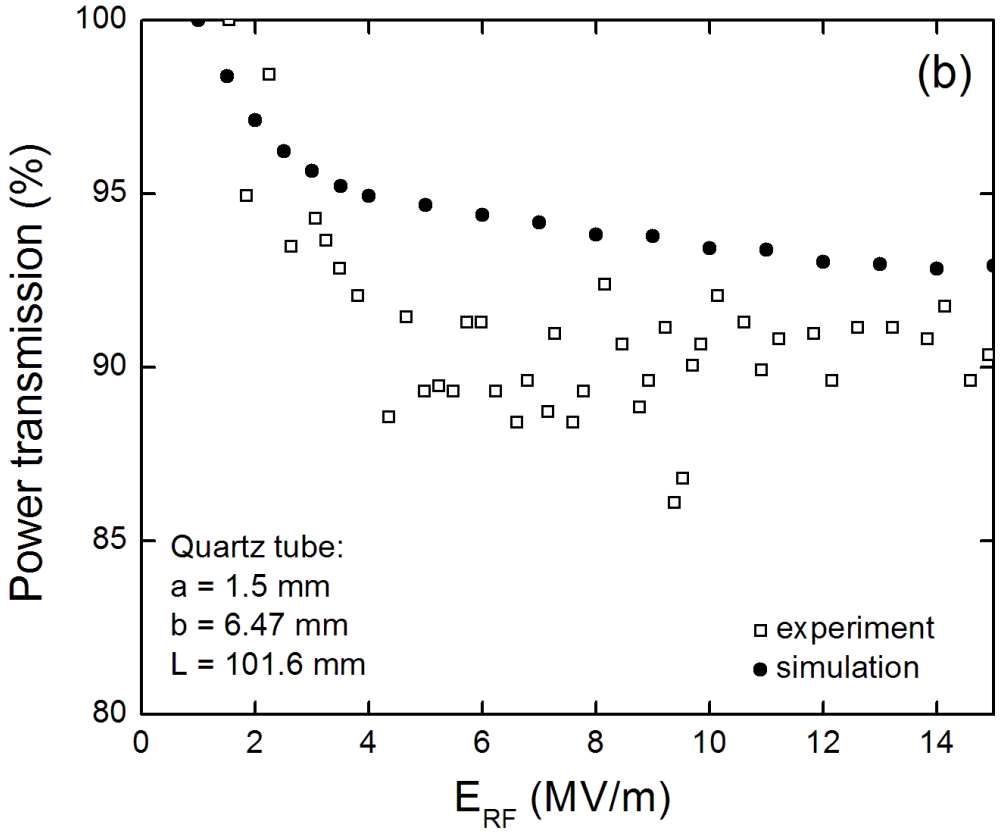

RF power transmission vs acceleration gradient for quartz-based DLA structure with inner diameter = 3 mm, SEY model: δ_{max0}= 2.4, E_{max0}=400 eV.

Summary

- We have developed a new 3-D self-consistent model of MP in DLA structures
- The model demonstrates very good agreement between simulations and experiment for different structure sizes
- We have shown that MP is driven by both radial and axial components of RF field and that effects of axial motion of particles cannot be neglected. They are particularly important when calculating MP-induced power loss in the structures with small inner diameter.

Future work

- More sophisticated Poisson solver to study the effects of SC non-uniformity
- More general analysis of MP for different structure types
- MP suppression by external magnetic field

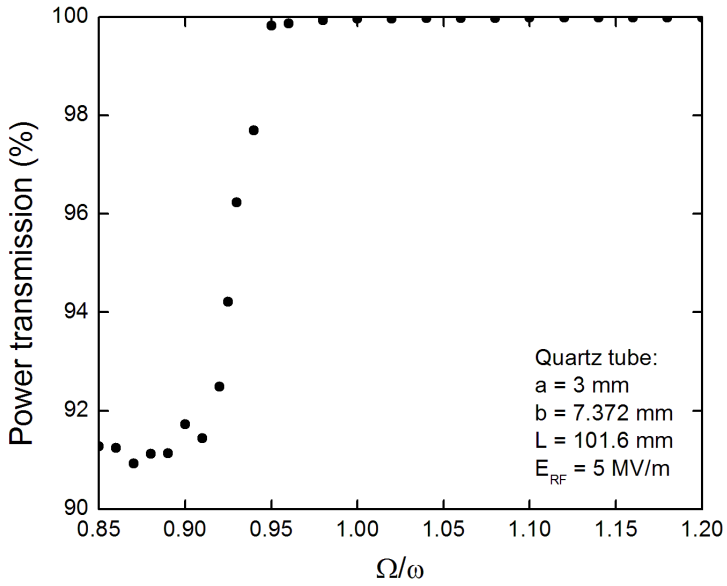

- Effects of grooves on the dielectric surface
- Standing wave structures

Acknowledgments

- This work is supported by the Office of High Energy Physics of the US Department of Energy.